Optical Loss Changes in Siloxane Polymer Waveguides During Thermal Curing

Shashikant G. Hegde,[1] Fuhan Liu,[2] Gee-Kung Chang,[2] Suresh K. Sitaraman[1]

[1]*Packaging Research Center, The George W. Woodruff School of Mechanical Engineering, Georgia Institute of Technology, Atlanta, Georgia 30332-0405*
[2]*School of Electrical and Computer Engineering, Georgia Institute of Technology, Atlanta, Georgia 30332-0405*

Received 6 September 2006; accepted 9 June 2007
DOI 10.1002/app.26945
Published online 25 July 2007 in Wiley InterScience (www.interscience.wiley.com).

ABSTRACT: The optical loss change in siloxane polymer waveguides during isothermal curing conditions is studied for the wavelengths of 850 and 1310 nm. As a first step, the evolution of degree-of-cure is determined from differential scanning calorimetry and compared to optical absorption from spectroscopy. It is found that the optical loss due to absorption mechanisms is related to the extent of cure reactions in the polymer. Optical loss due to scattering mechanisms is related to local density fluctuations, and is studied using dielectric analysis. Optical loss measurements are conducted on both uncladded and cladded waveguides during isothermal cure, which results in certain optical loss trends. Based on the trends, the underlying mechanisms for the optical loss variations are proposed and a cure schedule to realize the lowest optical loss is suggested. © 2007 Wiley Periodicals, Inc. J Appl Polym Sci 106: 2320–2327, 2007

Key words: optics; infrared spectroscopy; dielectric properties; polysiloxanes; differential scanning calorimetry

INTRODUCTION

Electrical interconnects at high speeds are limited by several factors such as frequency-dependent signal attenuation, crosstalk, high power consumption, jitter, and skew.[1] As data rates on backplanes and boards rise, optical interconnects at the backplane and board level are viewed as a potential technology solution for low power, high density, and high speed interconnects. Several optoelectronic packaging techniques using polymer waveguides are being developed to address electronic system needs.[2,3] Polymer waveguides are compatible with board-level processes and have lower processing temperature, making them an attractive option for enabling low-cost and high-density optical interconnects on board materials like epoxy glass FR4. However, the optical loss of waveguide polymers is much higher than that of silica used in optical fibers, and it is a significant contributor to the optical loss of the optoelectronic system. There are studies which have shown that different cure conditions can result in different values for optical loss in a polymer waveguide,[4–6] although there is no study which looks at the trend of the optical loss variation during curing and attribute it to several loss mechanisms. Such a study is useful in providing guidelines for the curing profile of an optical waveguide polymer to ensure lowest possible optical loss.

The chemical structure of the optical polymer studied in this research has a siloxane backbone (Si—O—Si) and organic side-chains. The curing reaction proceeds with a condensation of the silanol monomers. Lack of the exact chemical composition of the siloxane polymer makes the cure study in this research strictly phenomenological in nature. In this work, dynamic and isothermal differential scanning calorimetry (DSC) experiments were carried out to understand the evolution of the degree-of-cure (DOC) of the polymer. The DOC yields the extent of the cure reactions in the polymer and is related to the absorption mechanisms of optical loss. Spectroscopy measurements are done on bulk polymer samples to determine the change of this absorption during curing. The optical loss variations in a polymer waveguide during curing can also be attributed to several scattering mechanisms. It has been shown by Sakaguchi[7] that thermal annealing results in lower Rayleigh scattering loss in optical fibers. Therefore, local density fluctuations during curing that can affect scattering loss are monitored using dielectric analysis (DEA) technique in this work.

The polymer waveguides studied are multimode waveguides with a cross-section of 50 μm × 50 μm. Although these waveguides are intended for organic substrates, the process is still under development.[8] Instead waveguide arrays are fabricated on silicon

Correspondence to: S. K. Sitaraman (suresh.sitaraman@me.gatech.edu).

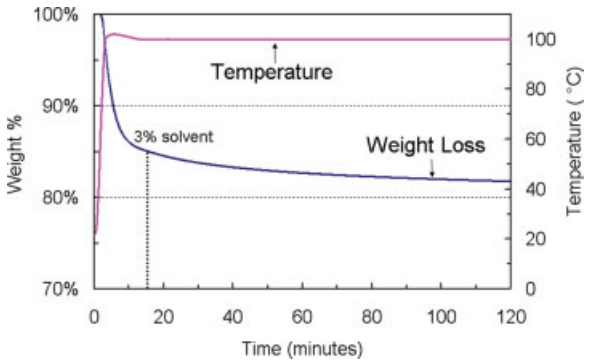

Figure 1 Isothermal TGA. [Color figure can be viewed in the online issue, which is available at www.interscience.wiley.com.]

substrates. The silicon substrate provides a smooth surface hence eliminating the need of a planarization or buffer layer on the substrate. Specific wavelengths of interest in this work are 850 nm and 1310 nm, which are typical emission wavelengths of datacom lasers for short link applications.[9] The optical loss of uncladded and cladded polymer waveguides is determined periodically during isothermal curing. Based on the trends, several loss mechanisms are proposed for the optical loss variations.

CURE KINETICS EXPERIMENTS

The siloxane optical polymer is supplied as both core and cladding types, which are very similar in composition, but with different refractive indices (n_{core} = 1.52; n_{clad} = 1.49). The curing experiments conducted in this work are on the core material, since the optical transmission in the waveguide is primarily contained in the core. As supplied, the core polymer is dissolved in solvent to enable deposition by spin coating. To evaluate the cure profile the first step is to remove all the solvent to get the accurate heat of the reaction. Since the material is photosensitive, UV exposure is required to release the catalyst that promotes polymerization. In exposed regions of the film, photo-generated acid catalyzes condensation of the silanols to initiate the polymer cross-linking. This is enough to insolubilize the material in an aqueous developer during waveguide fabrication; however further thermal cure is needed to fully build the network structure. This section evaluates the cure kinetics of the polymer during the final cure, which is done at the isothermal condition of 150°C.

To determine the isothermal prebaking condition and the solvent weight loss characteristics, the TA Instruments® 2050 thermogravimetric analyzer (TGA) was used. Several uncured and unexposed siloxane polymer samples of weights ranging from 10 to 15 mg were taken. Initially a dynamic scan was run at 5°C/min from room temperature to 200°C, and the change in sample weight was measured. The entire weight loss of 18%, which occurs before 120°C, is attributed to the presence of solvent. Isothermal TGA scan was run at the prebaking condition of 100°C, and the weight loss characteristics is shown in Figure 1. The weight of solvent remaining after the prebaking condition of 15 min is 3% and there is almost no solvent content after the prebaking condition of 80 min. Free-standing polymer samples of weights ranging from 7 to 12 mg were prepared using prebaking conditions of 15 min and 80 min in a convection oven. The samples were exposed to UV light of wavelength, λ = 340 nm and a dose of 3.8 J/cm^2 using a Tamarack Scientific® exposure tool. This UV exposure dose of 3.8 J/cm^2 is sufficient to provide photo-initiation for the different sample thicknesses used in the experiments in this work.

To get the heat of the cure reaction, DSC experiments were performed using TA Instruments® Q1000 with hermetically sealed aluminum pans. Care was also taken to minimize the time between UV exposure and subsequent DSC analysis. The dynamic heating rate experiments were conducted from room temperature to 200°C at a heating rate of 5°C /min. Illustrated in Figure 2 are the exothermic heat flow results for the different prebaking conditions, as a function of temperature. A subsequent dynamic scan was also done at 10°C/min to confirm that the samples had cured completely at the end of the first dynamic scan, and to determine the glass transition temperature. The modulation conditions used were temperature amplitude ±0.48°C and period 40 s. The glass transition temperature, T_g calculated from the midpoint in the step transition of reversible heat of the fully cured samples, was at 102°C ± 2°C. It must be noted that the glass transi-

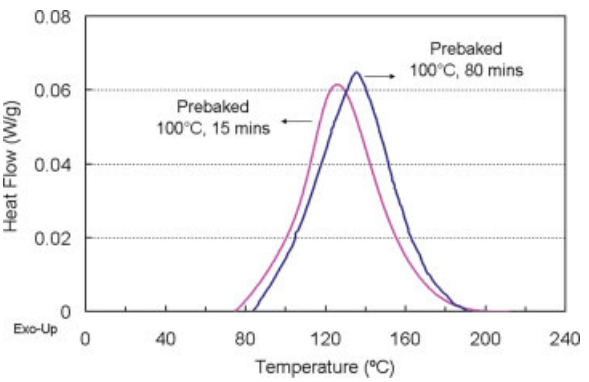

Figure 2 Dynamic DSC scans at different prebaking conditions (baseline corrected). [Color figure can be viewed in the online issue, which is available at www.interscience.wiley.com.]

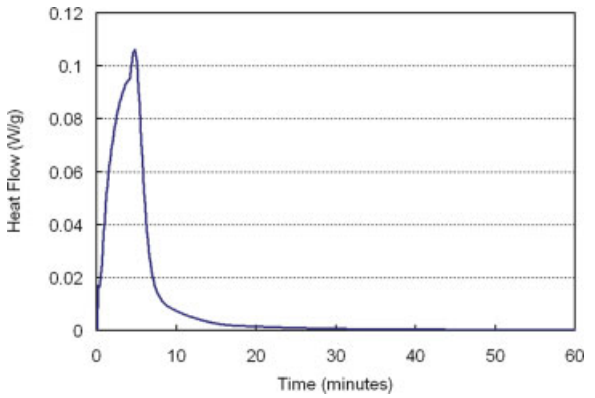

Figure 3 Isothermal DSC scan (baseline corrected). [Color figure can be viewed in the online issue, which is available at www.interscience.wiley.com.]

tion temperature indicated by DSC was very weak. The total enthalpy of the curing reaction or the ultimate heat of reaction, H_{ult} was calculated as 35.3 J/g for the 80-min prebaked sample, and was found to be similar to the 15-min prebaked sample. All the experiments conducted in the remainder of this work were done on 15-min prebaked samples, which correspond to the recommended prebake time from the supplier for this polymer at 100°C. A longer prebake time was not desired as it may affect other properties of the polymer, such as the photoinitiation. The 3% remaining solvent is not considered significant in these experiments, because the curing temperature of 150°C is significantly higher than the vaporization temperature of the solvent. The solvent will be lost within a minute or so of curing time, and therefore, the samples were not prebaked more than 15 min.

Isothermal DSC scans were performed on several samples that were already prebaked for 15 min and UV exposed. The scan was done at 150°C for duration of 60 min. Illustrated in Figure 3 is the heat flow exotherm from the isothermal experiment. A subsequent dynamic scan was done at 10°C/min on each of these samples to determine the residual heat of reaction, if any. No residual exotherm was observed in the subsequent dynamic scans. The T_g, calculated from the midpoint in the step transition of the fully cured samples, was at 105°C ± 2°C. This T_g is consistent with that obtained from dynamic DSC experiments. In Figure 3 there is a step or shoulder in the heat flow which may indicate a change in the rate-controlling step of the curing process.[10–12] Although in most polymer curing processes this indicates a change to a diffusion controlled reaction, it is not clear if this is the case here, due to the T_g of the polymer being lower than the isothermal curing temperature of 150°C. The polymer does not undergo vitrification in these curing experiments again since the final T_g of the polymer is significantly lower than the isothermal curing temperature of 150°C. The heat of reaction (H) at each point of the curing process is calculated from the area under the curve. The evolution of degree-of-cure (DOC) at the isothermal cure temperature 150°C, is calculated as DOC = H/H_{ult}, and shown in Figure 4. After 30 min of curing the DOC is 96%. Complete cure is achieved after 60 min of curing time. The reason for slow progress of cure at higher DOC is because of the diffusion-controlled nature of the cure reactions. It is important to emphasize that 100% cure of the waveguide polymer is not always desirable in sequential processing, since adhesion of the core polymer to the subsequent cladding polymer layers will deteriorate with a higher DOC.[13]

DIELECTRIC ANALYSIS

The variation in molecular orientation due to an electric field force is a very sensitive way of monitoring macroscopic changes in a polymer such as curing and viscosity. Dielectric analysis also has the particular advantage of being able to measure the changes *in situ*, as the polymer changes from a liquid with varying viscosity to a cross-linked insoluble solid. The dielectric parameter of interest is dielectric loss factor, ε'' which is the imaginary component of the complex dielectric permittivity, $\varepsilon^* = \varepsilon' - i\varepsilon''$, where ε' is the dielectric constant or relative permittivity. The ε'' of the polymer was measured using TA Instruments® dielectric analyzer, DEA 2970 with a single surface sensor having interdigitated electrodes. At the start of the analysis, the sensor was mounted into the furnace, and calibration was performed under nitrogen gas purge. The sensor was then taken out and uncured polymer was deposited onto the entire surface of sensor, such that it filled the spaces between the electrodes. The thickness of the sample on the sensor is around 1 mm, and is

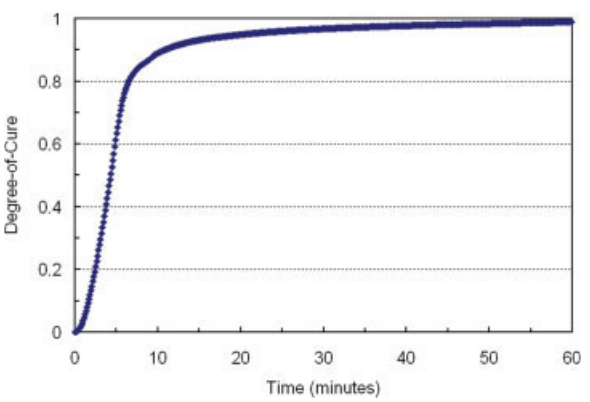

Figure 4 Evolution of DOC during isothermal cure. [Color figure can be viewed in the online issue, which is available at www.interscience.wiley.com.]

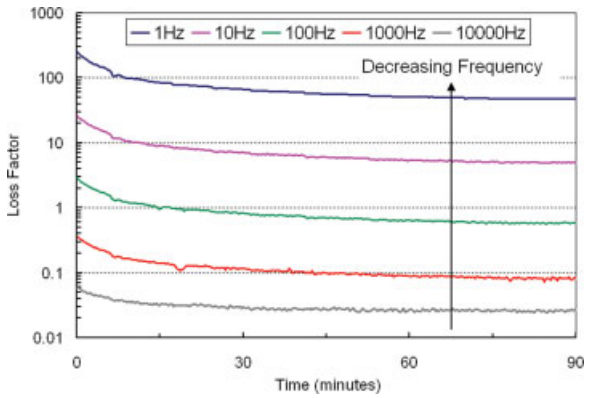

Figure 5 Dielectric loss factor during isothermal cure. [Color figure can be viewed in the online issue, which is available at www.interscience.wiley.com.]

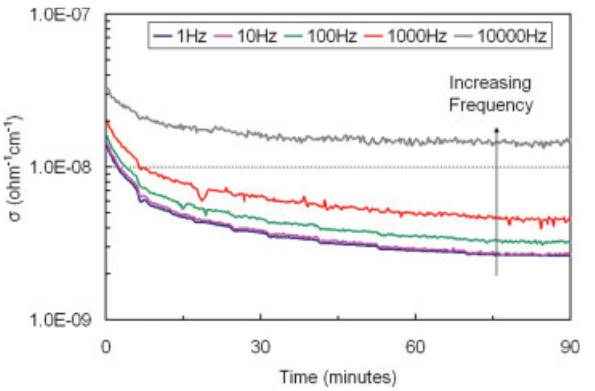

Figure 6 Ionic conductivity. [Color figure can be viewed in the online issue, which is available at www.interscience.wiley.com.]

comparable to the sample thickness in the DSC experiments. The sensor with the polymer was prebaked at 100°C for 15 min in a convection oven and UV exposed with the same conditions as the DSC experiments. The single surface sensor of the DEA 2970 is then mounted onto a heating chuck in the furnace. The chuck is then heated up rapidly and evenly to the isothermal temperature of 150°C. The dielectric analysis experiment was then conducted for over 80 min, as the polymer material was being cured. The dielectric loss factor ε'' was measured over a frequency range from 1 to 10,000 Hz. The frequency range was selected to allow measurement of 15 data points within a period of 1 min. This scanning rate is sufficiently short to assume the instantaneous snapshot of ε'' during the isothermal curing. The results of the measurement are shown in Figure 5. Dielectric loss factor consists of two parts $\varepsilon'' = \varepsilon''_{\text{ionic}} + \varepsilon''_{\text{dipole}}$, where $\varepsilon''_{\text{ionic}}$ is the contribution from ionic conductivity, and $\varepsilon''_{\text{dipole}}$ is the contribution from dipole relaxation. Studies have shown that $\varepsilon''_{\text{ionic}}$ is dominant at low frequencies and has an intrinsic character that involves ionic mobility of the molecules that react to form the polymer network.[14] The $\varepsilon''_{\text{dipole}}$ is dominant at higher frequencies and is due to the rotational mobility of bound charge.[15,16]

Ionic conductivity is the dielectric parameter with qualitative analogy to the mobility of polymer chains. Several methods have been reported to extract the ionic conductivity from measurements of ε'' and have been described in detail.[17,18] In this study, the method used is based on the ionic conductivity parameter σ (ohm^{-1} cm^{-1}) = $\varepsilon_o \omega \varepsilon''$, where ε_o is the dielectric constant of vacuum. At certain low-frequencies the σ values overlap, and can be used as a measure of the change of ionic conductivity with isothermal curing time.[15] Figure 6 shows the variation in the σ parameter during isothermal curing at 150°C. The overlapping values of σ at 1 Hz and 10 Hz can be taken as the ionic conductivity of the polymer. As the cure reaction proceeds, the cross-linking and increasing molecular weight of the chains rapidly increases viscosity. As a consequence the ionic mobility is restricted leading to a decrease in σ.

Among the various relationship between the cure evolution and the ionic conductivity, the one proposed by Day,[19] is used here which normalizes the ionic conductivity as a cure index with the following equation:

$$\text{Cure index } (t) = \frac{\log \sigma(t) - \log \sigma_{0\%}}{\log \sigma_{100\%} - \log \sigma_{0\%}} \qquad (1)$$

where, t is the curing time, $\sigma_{0\%}$ is the ionic conductivity at the start of curing, and $\sigma_{100\%}$ is the stabilized value of ionic conductivity at the end of curing. Figure 7 shows the evolution of cure index and DOC with isothermal curing time for the polymer. Although the trends are similar, it is seen that the evolution of cure index significantly lags the DOC of the reaction. Similar differences in evolution of cure

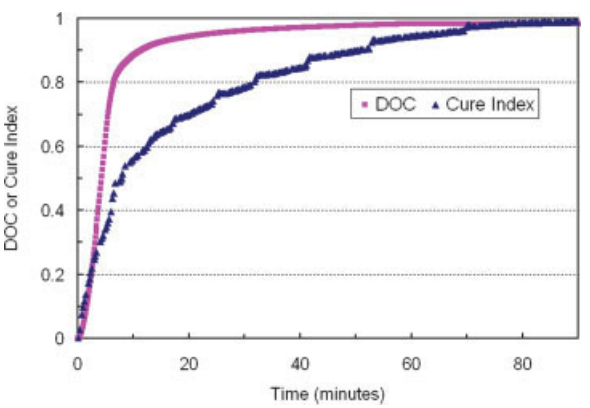

Figure 7 Evolution of cure index during isothermal cure. [Color figure can be viewed in the online issue, which is available at www.interscience.wiley.com.]

TABLE I
Optical Loss Mechanisms in Polymer Waveguides

Absorption	Scattering
Intrinsic Factors	
Vibration overtones	Rayleigh scattering
Electronic transitions	
Extrinsic Factors	
Absorbed water	Inhomogeneities
Contaminants	Core/cladding interface
	Voids, cracks

index and DOC have been observed by others.[14,20] The DOC reaches 96% after 30 min of curing however the curing index is only 80%. It is important to note that the isothermal curing temperature of 150°C is significantly higher than the T_g, of the fully cured polymer. This suggests that the likely reason for ionic conductivity changes after late stages of cure is due to the continued mobility of the polymer chains. This process affects the local density fluctuations in the polymer and can change the optical loss in the polymer waveguide, as will be discussed in the next section. The cure index reaches 100% at around 80 min of isothermal cure, which indicates that the mobility of the polymer chains has saturated.

OPTICAL LOSS MECHANISMS

Optical loss mechanisms in polymer waveguides can be divided into intrinsic and extrinsic loss factors as shown in Table I. Similar loss mechanisms have been previously described for other polymer interconnects.[21] For purpose of illustration, a schematic of the optical loss in dB/cm is shown in Figure 8, along the visible wavelength region (400 to 700 nm) and the near infrared wavelength region (700 to 1600 nm). The wavelengths of 850 and 1310 nm lie in regions with relatively lower optical loss.

The intrinsic mechanisms include absorption peaks due to vibration overtones. These are fundamental absorptions from molecular bonds such as Si—O and other organic bonds in the siloxane polymer, and are found throughout the near infrared region. The other intrinsic absorption mechanism is electronic transition absorption, which varies with wavelength as $1/\lambda$, where λ is the wavelength. Electronic transition absorption is present primarily in the wavelength regions < 700 nm. It is not much of a concern in our study because our wavelengths of interest do not lie in that range. Absorption in the polymer can also be due to external impurities or from absorbed water. All the absorption mechanisms can be detected by spectroscopy analysis as changes in absorption peaks.

The scattering losses are equally as important as absorption loss in polymer waveguides. The intrinsic scattering mechanism is called Rayleigh scattering, and occurs due to local density fluctuations in the polymer. During the process, the energy of the incident photon is conserved; however its propagating direction is changed, resulting in possible loss of light into the cladding of the waveguide. Rayleigh scattering varies with wavelength as $1/\lambda^4$. Extrinsic scattering mechanisms develop as a consequence of the fabrication process of the polymer waveguide. During the fabrication process many imperfections may develop such as inhomogeneities, core-cladding interface roughness, micro-voids and micro-cracks. These imperfections increase the optical loss by light scattering, independent of wavelength.[21,22] Extrinsic scattering mechanisms are much harder to detect and distinguish from other types of losses. Although there have been studies on them, they are also not easy to quantify.[23,24]

SPECTROSCOPY ANALYSIS

The changes in optical absorption of the siloxane polymer during curing have been monitored using Cary® 5E dual-beam spectrophotometer in the visible (400 to 700 nm) and near-infrared regions (700 to 1900 nm). Several samples in the form of bulk polymer slabs of thickness 2 mm are used. The spectroscopy samples are prepared using the same process conditions as the DSC and DEA experiments, which includes a prebaking time of 100°C for 15 min, and UV exposure dose of 3.8 J/cm^2. The absorbance is measured in absorbance units (au). The absorbance (A) for a sample of thickness (t) can be converted to optical absorption loss (α_{abs}) in units of dB/cm by using the formula $\alpha_{abs} = (10A)/t$. Figure 9 shows the absorbance of the siloxane polymer sample in four different stages; uncured, 15 min cured, 30 min cured, and 60 min cured.

It is seen from the spectroscopy result that after the polymer is cured for 15 min the absorption loss

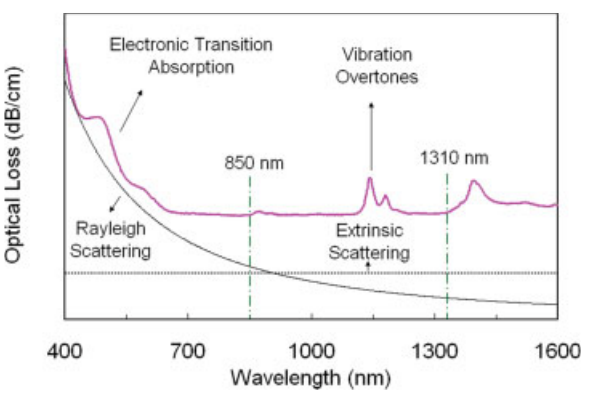

Figure 8 Optical loss mechanisms shown along wavelength spectrum. [Color figure can be viewed in the online issue, which is available at www.interscience.wiley.com.]

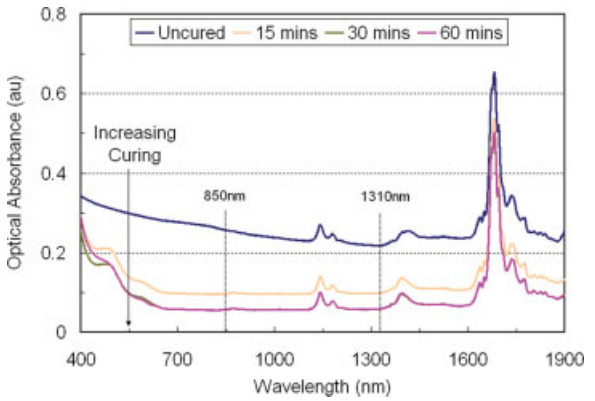

Figure 9 Absorption spectrum changes. [Color figure can be viewed in the online issue, which is available at www.interscience.wiley.com.]

has substantially decreased compared to its uncured state. The measurements taken at 30 and 60 min coincide except for the wavelength region between 400 and 500 nm where there is a slight increase in optical absorption for the 60-min sample. These trends were confirmed for several samples. The wavelength range between 400 and 500 nm corresponds to the electronic transition absorption, and any increase could mean that there is slight oxidation that occurs along with curing.[25] Another noticeable change during curing is the decrease in the absorption peak at 1400 nm. This peak corresponds to vibration overtones of the hydroxyl bond O—H, and its reduction is a consequence of the condensation reaction during curing.

For the wavelengths 850 and 1310 nm the results show that the polymer reaches its minimum optical absorption loss after 30 min, which corresponds to a DOC of 96%. This is expected since the absorption optical loss corresponds to the chemical changes that are occurring during curing. Any further change in absorption optical loss beyond 30 min of curing is likely so small that it is not detectable by the spectrometer. The spectroscopy results reveal no additional peaks being formed during curing, near the wavelengths of 850 and 1310 nm. This suggests that any extrinsic absorption mechanism, from moisture or contaminants, is not present during curing.

OPTICAL LOSS IN WAVEGUIDES

To investigate the optical loss changes in waveguides, two sets of waveguide samples were fabricated on silicon substrate. The first set of samples is without a top clad and is called uncladded sample. The second set of samples is with a top clad and is called cladded sample. Each sample has an array of five waveguides as shown in the schematic in Figure 10.

The fabrication steps include initially spin coating the cladding polymer of refractive index 1.49 on the silicon wafer. As recommended by the supplier, this bottom cladding polymer layer was prebaked at 90°C for 10 min. The cladding polymer is not photosensitive, and can be directly thermally cured at 150°C for 60 min in a convection oven without the need for any UV exposure. In the sample fabrication process, the bottom cladding polymer layer was partially cured at 150°C for 30 min in a convection oven. Full cure of the cladding polymer is not desired because it will lower its adhesion with the core polymer. The core polymer with a refractive index 1.52 is then spin coated on top of the cladding layer. The spinning process is controlled to give a thickness of 50 μm for the core layer. The core polymer is prebaked at 100°C for 15 min. The core polymer is then UV exposed using a glass mask to photodefine the waveguide. The resulting waveguides have a cross-section of 50 μm × 50 μm and have lengths ranging 4 to 5 cm. However, at this time the waveguides is in an uncured condition. The fabrication of the waveguide samples without a top clad layer is stopped here, while the samples with a top clad have an additional layer of cladding polymer spin coated on top of the core polymer waveguide.

For the uncladded samples, the wafers with the partially-cured bottom cladding layer and the prebaked and UV-exposed core layer were subjected to a thermal cure at 150°C, and optical loss measurements were then performed over 90 min. For the cladded samples, the wafers with the partially-cured bottom cladding layer, prebaked and UV-exposed core layer, and spin-coated uncured top cladding layer were subjected to a thermal cure at 150°C, and optical loss measurements were then performed over 90 min. Although the surrounding cladding layers are being cured in addition to the core polymer material, the optical transmission is confined within the core polymer during this curing process, as the core polymer has a higher refractive index compared to the cladding layers. Therefore, the measured optical loss is assumed to be a function of the DOC of the core polymer, and not influenced by the curing of the surrounding cladding polymers.

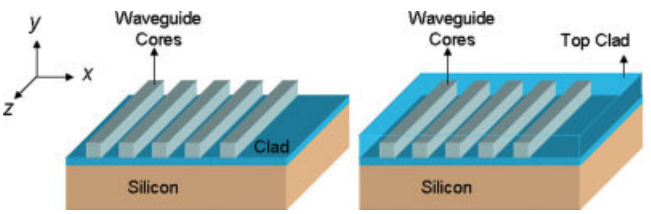

Figure 10 Schematics of uncladded and cladded samples. [Color figure can be viewed in the online issue, which is available at www.interscience.wiley.com.]

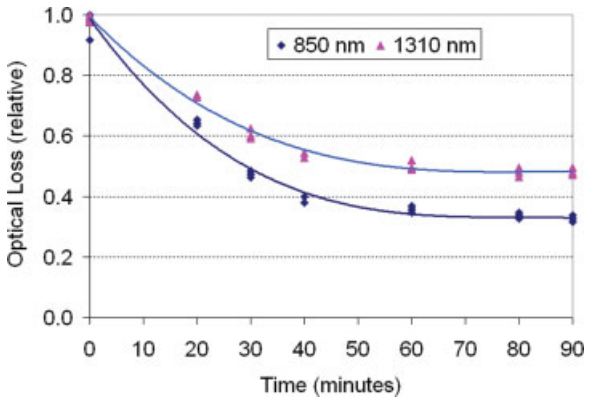

Figure 11 Relative optical loss change for uncladded waveguides during isothermal cure. [Color figure can be viewed in the online issue, which is available at www.interscience.wiley.com.]

To measure optical loss, a continuous wave power from an external laser at wavelengths 850 and 1310 nm is launched into the polished end face of the waveguide from a cleaved single-mode fiber. At the waveguide output face, also polished, the transmitted power is coupled into a cleaved multi-mode fiber and measured by a calibrated optical power detector. The two fibers are individually held and manually positioned by bare fiber holders in 5-axes (x, y, z, θ_x, θ_y). Care must be taken to precisely adjust the alignment between fibers and the waveguide to obtain the maximum coupling efficiency. The waveguide optical loss per unit length is defined as:

$$\alpha = \frac{10}{l} \log\left(\frac{P_{\text{input}}}{P_{\text{output}}}\right) \tag{2}$$

where, P is the power and l is the length of the waveguide in centimeters. Using the coupling scheme and experimental set-up described, the waveguide optical loss was measured. The samples were cured in a convection oven at a temperature of 150°C and the optical loss, α was monitored at certain intervals of curing, until the variations of optical loss stabilized. The relative optical loss change for uncladded waveguides is shown in Figure 11, for wavelengths of 850 and 1310 nm. The optical loss change, $\Delta\alpha$ after 30 min of curing is 53% at 850 nm and 40% at 1310 nm. The relative optical loss change for cladded waveguides is shown in Figure 12, for wavelengths of 850 nm and 1310. The optical loss change, $\Delta\alpha$ after 30 min of curing is 60% at 850 nm and 54% at 1310 nm.

As expected from previous observations in spectroscopy, the optical loss decreases during curing due to a decrease in absorption. However, unlike the spectroscopy results the waveguide optical loss continues to decrease beyond the curing time of 30 min. There is also some decrease in optical loss after the polymer has reached a DOC of 100% at 60 min of curing, more evident in the case of cladded waveguides. The optical loss changes finally stabilize at around 80 min of curing. The $\Delta\alpha$ for uncladded waveguides after 80 min of curing is 65% at 850 nm and 54% at 1310 nm. The $\Delta\alpha$ for cladded waveguides after 80 min of curing is 90% at 850 nm and 77% at 1310 nm.

At a curing time of 30 min most of the chemical reactions in the polymer have taken place. Since $\Delta\alpha$ continues to change well beyond 30 min of curing, it is certain that the absorption loss is not the only factor causing $\Delta\alpha$. Furthermore, extrinsic scattering due to micro-cracks and micro-voids can be excluded, since they would only increase the optical loss, and cannot explain the trends that were obtained. The most likely scattering mechanisms that are causing the decrease in optical loss beyond 30 min of curing are Rayleigh scattering and extrinsic scattering due to inhomogeneities. From the dielectric analysis it was found that the cure index is only 80% at a curing time of 30 min. Further curing leads to a reduction of polymer chain mobility which can reduce both Rayleigh scattering due to local density fluctuations as well as reduce inhomogeneities. Practically it is very difficult to separately identify the contributions of the two scattering mechanisms. If the optical loss change due to Rayleigh scattering is taken as $\Delta\alpha_{\text{ray}}$, and the optical loss change due to inhomogeneities is taken as $\Delta\alpha_{\text{inh}}$, then $\Delta\alpha$ during waveguide curing can then be expressed as:

$$\Delta\alpha = \Delta\alpha_{\text{abs}} + \Delta\alpha_{\text{ray}} + \Delta\alpha_{\text{inh}} \tag{3}$$

The cladded waveguides show a much sharper decrease in optical loss compared to uncladded waveguides during curing because of several reasons; the core shape is maintained better during curing, lower scattering loss due to smoother sidewalls,

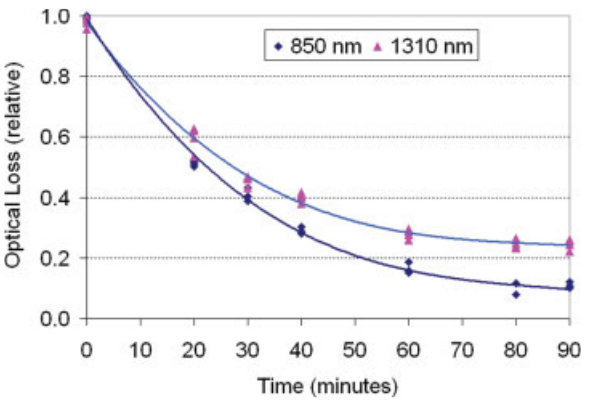

Figure 12 Relative optical loss change for cladded waveguides during isothermal cure. [Color figure can be viewed in the online issue, which is available at www.interscience.wiley.com.]

no effect of dust particles, and finally they are less prone to physical damage. It must be noted that there can be differences in optical loss trends in other types of polymers such as polycyanurates described in Dreyer et al.,[6] where the optical loss of the cured polymer is actually higher than the monomers. The optical loss trends described in this article will hold for most waveguide materials where absorption loss decreases with the evolution of DOC.

One interesting aspect of the optical loss change in the waveguides is that the trend is similar to the cure index evolution. Since the cure index incorporates effects of both chemical cure as well as compositional variations in the polymer it could potentially be used as an indicator for optical loss changes. Although this work focuses on optical loss during curing at 150°C, the conclusions drawn can be applied to curing at different temperatures as well. At lower temperatures, the evolution of DOC will be different, and depending on the temperature, 100% cure may not be even possible. However, the inherent optical loss mechanisms such as absorption and scattering loss, discussed in this work, will still be applicable at other temperatures as well.

CONCLUSIONS

The optical loss change in siloxane polymer waveguides during isothermal curing conditions of 150°C is studied for the wavelengths of 850 and 1310 nm. The optical loss mechanisms responsible for the decrease in optical loss during curing of polymer waveguides have been identified as absorption loss, Rayleigh scattering and extrinsic scattering. It has been shown that complete curing of the polymer waveguide did not result in the minimum optical loss. Further annealing was required to ensure that all the scattering mechanisms have stabilized. In the siloxane waveguides this occurs at around 80 min of isothermal curing at 150°C. The optical loss decrease in cladded waveguides is more than in uncladded waveguides mainly because the core shape is maintained during curing. Such a study is useful to provide guidelines for curing profile of the polymer, which ensures that the optical loss of the waveguide has attained its least possible value.

References

1. Miller, D. A. B. Proc IEEE 2000, 88, 728.
2. Sang-Yeon, C.; Brooke, M. A.; Jokerst, N. M. IEEE J Selected Top Quantum Electronics 2003, 9, 465.
3. Shimokawa, F.; Koike, S.; Matsuura, T. In Proc IEEE Electronic Components and Technology Conference, 1993, pp 705–710.
4. Kowalczyk, T. C.; Kosc, T.; Singer, K. D.; Cahill, P. A.; Seager, C. H.; Meinhardt, M. B.; Beuhler, A. J.; Wargowski, D. A. J Appl Phys 1994, 76, 2505.
5. Reuter, R.; Franke, H.; Feger, C. Appl Opt 1988, 27, 4565.
6. Dreyer, C.; Bauer, M.; Bauer, J.; Keil, N.; Yao, H.; Zawadzki, C. Microsyst Technol 2002, 7, 229.
7. Sakaguchi, S. Electronics Commun Japan Ii-Electronics 2000, 83, 35.
8. Chang, G. K.; Guidotti, D.; Liu, F.; Chang, Y. J.; Zhaoran, H.; Sundaram, V.; Balaraman, D.; Hegde, S.; Tummala, R. R. IEEE Trans Adv Packaging 2004, 27, 386.
9. Uhligand, S.; Robertsson, M. J Lightwave Technol 2006, 24, 1710.
10. Amendola, E.; Carfagna, C.; Giamberini, M.; Pisaniello, G. Macromol Chem Phys 1995, 196, 1577.
11. Carfagna, C.; Amendola, E.; Giamberini, M.; Filippov, A. G.; Bauer, R. S. Liquid Crystals 1993, 13, 571.
12. Vyazovkin, S.; Mititelu, A.; Sbirrazzuoli, N. Macromol Rapid Commun 2003, 24, 1060.
13. Strandjord, A. J. G.; Garrou, P. E.; Heistand, R. H.; Tessier, T. G. IEEE Trans Components Packaging Manuf Technol B Adv Packaging 1995, 18, 269.
14. Bellucci, F.; Valentino, M.; Monetta, T.; Nicodemo, L.; Kenny, J.; Nicolais, L.; Mijovic, J. J Polym Sci Part B: Polym Phys 1995, 33, 433.
15. Kranbuehl, D.; Hood, D.; Rogozinski, J.; Meyer, A.; Neag, A. Prog Org Coatings 1999, 35, 101.
16. Kim, H.; Char, K. Bull Korean Chem Soc 1999, 20, 1329.
17. Senturia, S. D.; Sheppard, N. F. Adv Polym Sci 1986, 80, 1.
18. Mangion, M. B. M.; Johari, G. P. Polymer (UK) 1991, 32, 2747.
19. Day, D. R. Polym Eng Sci 1989, 29, 334.
20. Stephan, F.; Fit, A.; Duteurtre, X. Polym Eng Sci 1997, 37, 436.
21. Kaino, T. J Polym Sci Part A: Polym Chem 1987, 25, 37.
22. Pirasteh, P.; Charrier, J.; Dumeige, Y.; Joubert, P.; Haesaert, S.; Chaillou, A.; Haji, L.; Le Rendu, P.; Nguyen, T. P. Phys Status Solidi A Appl Mater Sci 2005, 202, 1712.
23. Ladouceur, F. J Lightwave Technol 1997, 15, 1020.
24. Dugas, J.; Maurel, G. Appl Opt 1992, 31, 5069.
25. Takezawa, Y.; Tanno, S.; Taketani, N.; Ohara, S.; Asano, H. J Appl Polym Sci 1991, 42, 2811.